Wasit Journal for Pure Science

Journal Homepage: https://wjps.uowasit.edu.iq/index.php/wjps/index
e-ISSN: 2790-5241 p-ISSN: 2790-5233

Three Dimensions of Fan Reconnection

Mohammed Qassim Moussa[1]*, Ali Khalaf Hussain[2]

[1,2]Department of Mathematics, College of Education for Pure Science, Wassit university, IRAQ

*Corresponding Author: Mohammed Qassim Moussa

DOI: https://doi.org/ 10.31185/wjps.416
Received 01 May 2024; Accepted 19 Jun 2024; Available online 30 Jun 2024

ABSTRACT: Many celestial occurrences, including solar flares and the solar corona and modifications to the magnetosphere of Earth, are thought to be caused by the reconnection process. This process occurs in highly conductive plasmas. One of the candidate places for this process is the three-dimensional zero points, in this process, stored energy is transformed into new types of energy

Aims. Magnetic reconnection at a single null point: influence of magnetic field symmetry.
Methods. We discussed a stable solution to several of the resistivity MHD formulations.

Results. The field's asymmetry (k) may impact the propagation area dimensions and rate of reconnection in a variety of ways, depending on the parameters we choose.

Keywords: MHD equation, Magnetic reconnection, current, plasma stream

1. INTRODUCTION

The magnetic reconnection operation involves breaking and reconnecting the field lines of two opposite magnetic fields and producing new lines. This causes a shift in the magnetic field's structure or geometry. In previous years, this process has been studied by many scientists and in many studies.

One of these investigations is an order-of-magnitude study, similar to the Sweet-Parker framework, in which a current plate (with length equivalent to the global outer long-scale) is situated between magnetic fields pointing in opposing directions. (Sweet, 1958), (Parker, 1957) [1],[2]. Sudden violent events such as CMEs and related occurrences on other star systems and solar flares (Parker, 1963) [3]. (Petschek, 1964) proposed that sluggish MHD waves would greatly reduce the area of the propagation zone and hence boost the reconnection pace [4]. Thus, the temperature of the corona rises to very high temperatures, exceeding millions of degrees (*e.g*., Parker, 1983) [5]. The Earth's magnetosphere (where satellites have seen reconnection sites, especially for non-terrestrial events.) when reacts with the winds from the sun (Xiao *et al*., 2006) [6], As well as in the atmospheres of other planets that have a magnetic nature (Al-Hachami *et al.*, 2010) [7]. The next sections will go over the significance of magnetic flux and its influence on reconnection. We will also show the mathematical model used to describe this phenomenon, and we will study the characteristics of the solution used for this model, especially (the nature of reconnection and the rate of reconnection). Then in conclusion, we will study and demonstrate the results we have achieved.

2. THE EFFECT OF MAGNETIC FLUX ON RECONNECTION

Several parts of plasma physics involve reorganizing the B magnetic field. When null points exist, the overall topology of the field changes. Our understanding of this reorganization is mostly based on the well-researched instance of two-dimensional reconnection. With a two-dimensional magnetic field, reconnection takes place at the null points Hyperbolic (see, *e.g.*, Priest and Forbes, 2000, for a review) [8], often referred to as X-points (see Fig. 1).

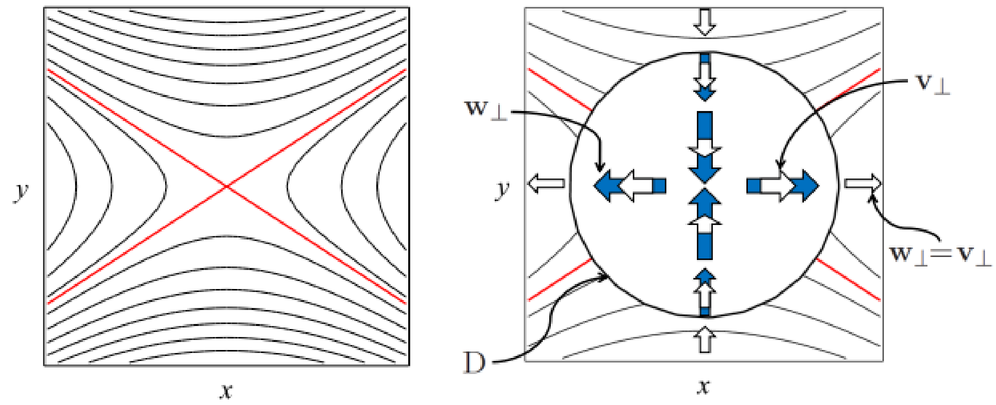

Figure 1 **over the right side of the picture is a schematic depicting the distinction among the plasma velocity (white arrows superimposed over the blue arrows representing flux transport) and the flux transporting velocity (blue arrows) inside a localized, non-ideal area (D). Near a hyperbolic two-dimensional null point (X-point), the field line structure is shown on the left. These separatrices, which are shown in red, divide the domain into four distinct topological areas**

When reconnection occurs at the X-point, a plasma stream carries the flux of magnetism there; thereafter, the flow carries the rejoining flux away from the X-point. The process of reconnection includes the convergence of a pair of magnetic field lines originating from two quadrants located on opposing sides of the null point. Along the field dividers, every line of field lines is interrupted at X-point. Then the new lines are organized together and exit in **B**'s last two quadrants. The result is that the resulting field lines are connected in a pairwise manner, different from when they left the reconnection area. Therefore, the (magnetic reconnection process) is considered a non-ideal process because the field lines do not maintain their identity, while it is assumed that in an ideal plasma, the field lines must Preserving their identity. The (non-ideality) may be caused by a non-zero resistance η, and in this case we assume that there are no effects. Other non-idealities According to this concept, Ohm's law satisfies this process and form

$$\boldsymbol{E} + \boldsymbol{v} \times \boldsymbol{B} = \boldsymbol{\eta J} \qquad (1)$$

To analyze the development of magnetic flux, it is important to establish a flux transport velocity $\boldsymbol{w}$ (Hornig and Schindler, 1996; Hornig and Priest, 2003) [9], [10]. which satisfies

$$\boldsymbol{E} + \boldsymbol{w} \times \boldsymbol{B} = 0 \qquad (2)$$

This is conceivable in two dimensions because the electric field, **E**, is always orthogonal to **B**. Keep in mind that reconnection can only occur if (the flux carrying velocity **w)** at the null point becomes single, a feature that indicates the field lines have broken and a follow-up discontinuity in the translation of their endpoints (Hornig, 2001) [11]. We may think of **w**as a flow in which the magnetic flux is fixed by comparing it to an ideal Ohm's law. The component of **w** that is orthogonal to **B** may be found. by looking at $\boldsymbol{w}_{\perp}$

$$\boldsymbol{w}_{\perp} = \boldsymbol{E} \times \boldsymbol{B}/B^2 \qquad (3)$$

To the right of Eq. (1), if we assume that the non-ideal term is determined within a certain region of D around the null point, And then outside D, The plasma velocity orthogonal to **B** coincide with $\mathbf{W}$,$\boldsymbol{v}_{\perp}$. Things are trickier when seen in three dimensions There is often no unique flux-conserving velocity, or more precisely, field lines running through D have no distinct field line velocity, for three-dimensional reconnection because **E.B** or **J.B** is typically non-zero inside a limited area D (to a proof, see Hornig and Schindler, *1996*; Priest et al., *2003*)[9] [12]. However, under certain conditions, it is still feasible to track the development of field lines and magnetic flux. Picture a resistive, Imperfect term η**J** contained inside a spreading area D. Given the very high magnetic Reynolds numbers of astrophysical plasmas and the fact that dissipation is more effective in locally concentrated areas, we assume that Limited area D represents the general case for astrophysical plasmas.

3. MATHEMATICAL MODEL

Research into magnetic reconnection is in its infancy because of the complexity of the topic. As a result, a simplified version of the MHD equations is one tool used to investigate this process's characteristics. Several 3-dimensional analytical solutions are detailed by (Hornig and Priest *2003*) and (Wilmot-Smith *et al*. 2006 and Al-Hachami 2019) [9],[13], [14] When there is not a null point in the magnetic field, and also solutions with the existence of a null.

(Pontin *et al.*, 2004, 2005; Priest and Pontin, 2009) [15],[16],[17]. These solutions satisfy the induction equations in addition to Maxwell's equations because they are from kinetic reconnection. This method can help us understand a lot about the nature of the magnetic reconnection process that happens in a separate diffusion area. (Schindler et al., 1988) [18]. We will look at the properties of the answers to this portion of the equations for MHD in the next chapter. Then we will look at which properties are still true when the MHD equations for the whole set of resistors are resolved.

In the empty magnetic point area, we are looking for a solution to MHD motor equations, so we replace

$$\mathbf{E} + \mathbf{v}\times \mathbf{B} = \eta\ \mathbf{J}, \tag{4}$$
$$\nabla\times \mathbf{E} = 0, \tag{5}$$
$$\nabla\times \mathbf{B} = \eta\ \mathbf{J}, \tag{6}$$
$$\nabla \cdot \mathbf{B} = 0. \tag{7}$$

Here, we often think of a zero point where the current is Collimated to the fan plane. The magnetic field that we settle on is

$$\boldsymbol{B_r} = \frac{B_0}{L}\left(\frac{2r\cos(\theta)^2+2\sin(\theta)jz+2\sin(\theta)ky}{k+1}\right) \tag{8}$$
$$\boldsymbol{B_\theta} = \frac{B_0}{L}\left(-\frac{2\cos(\theta)(r\sin(\theta)-jz-ky)}{k+1}\right) \tag{9}$$
$$\boldsymbol{B} = \frac{B_0}{L}\ \frac{2}{k+1}\ (x, ky-jz, -(k+1)z) \tag{10}$$

where B_0, L and j are constants. The field's cylindrical symmetry makes it easy to Application in Cartesian coordinates (x, y, and z), where B has the form

$$\boldsymbol{B_x} = \frac{B_0}{L}\frac{2}{k+1}x \tag{11}$$
$$\boldsymbol{B_y} = \frac{B_0}{L}\frac{2}{k+1}(ky-jz) \tag{12}$$
$$\boldsymbol{B_z} = \frac{B_0}{L}\frac{-2(k+1)}{k+1}z \tag{13}$$

where k is a parameter, and we limit our attention to the scenario when j and k are greater than 0. This expands upon the earlier study by (Pontin et al. 2005), which only examined the scenario in It has azimuthally identical field in the fan plane (z = 0)., leading to k = 1 [15].

Along the x-axis, we have the current, which is determined by

$$\boldsymbol{J} = \frac{2B_0}{\eta L(k+1)}(j, 0,0),$$

from Eq. (6). To determine the magnetic structure around a null point locally, we presuppose a magnetic field next to the null point, where the field vanishes (**B**=0).

We take it as read that Each and every eigenvalue is genuine. examination of (the Jacobian matrix **M)**

The null point's eigenvalues are determined to be

$\lambda_1 = \frac{2B_0}{L(k+1)}$ $\qquad$ $\lambda_2 = k(\frac{2B_0}{L(k+1)})$ $\qquad$ $\lambda_3 = -(k_+1)\left(\frac{2B_0}{L(k+1)}\right)$

With identical eigenvectors

$\boldsymbol{k_1} = (1,0,0)$ $\qquad$ $\boldsymbol{k_2} = (0,1,0)$ $\qquad$ $\boldsymbol{k_3} = \left(0,1,\frac{2p+1}{j}\right)$

From the image above with little doubt, $k_1$and $k_2$make up the fan plane (because k > 0) given that they conform to the identical indication eigenvalue of **M**. (Parnell et al., 1996) [19]. While the spine is perpendicular to the plan z=0, This magnetic null point's fan plan is consistent with it, nonetheless, it instead lies along

$x = 0$ $\qquad$ $y = jz/(2k+1)$ $\qquad$ (see figure 2)

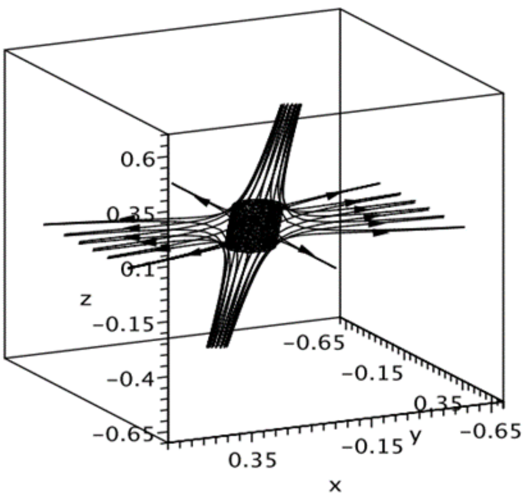

(a)

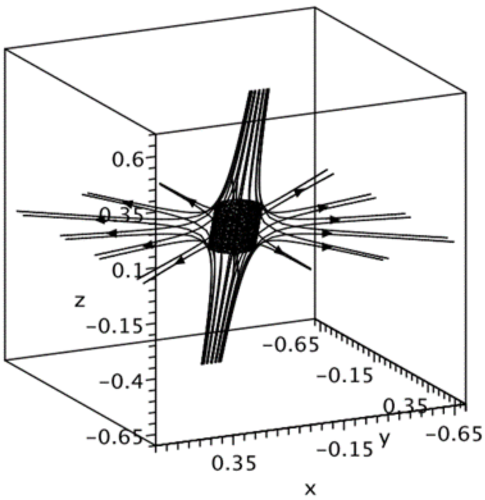

(b)

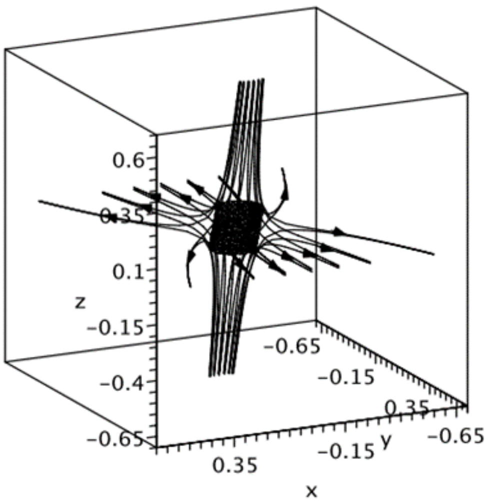

(c)

Figure 2: The magnetic null point configuration for j= 1 and varied values of k: (a)k = 0.5, (b) k = 1 and (c) k = 2. The diffusion region's form is shown by the shaded cylinder.

Regarding the chosen magnetic field (10) The equation of the lines of magnetic field may be expressed in closed form, by solving

$$\frac{\partial \mathbf{X}(s)}{\partial s} = \mathbf{B}\big(\mathbf{X}(s)\big), \tag{14}$$

When the term s runs along field lines, to give

$$x = x_o e^{\left(\frac{2B_0}{L(k+1)}\right)s} \tag{15}$$

$$y = \left(y_o - \frac{jz_o}{2k+1}\right) e^{k\left(\frac{2B_0}{L(k+1)}\right)s} + \frac{jz_o}{2k+1} e^{-\frac{2B_0 s}{L}} \tag{16}$$

$$z = z_o e^{-\frac{2B_0 s}{L}} \tag{17}$$

The inverse of Eqs. (15, 16, 17) are

$$x_o = x e^{-\left(\frac{2B_0}{L(k+1)}\right)s} \tag{18}$$

$$y_o = \left(y - \frac{jz}{2k+1}\right) e^{-k\left(\frac{2B_0}{L(k+1)}\right)s} + \frac{jz}{2k+1} e^{\frac{2B_0 s}{L}} \qquad (19)$$

$$z_o = ze^{\frac{2B_0 s}{L}} \qquad (20)$$

The equations of the lines of magnetic fields under certain initial coordinates $\mathbf{X_0} = (x_0, y_0, z_0$are shown. We go on to resolve Eqs. (4-7) as follows. From Eq. (5) In general we can write,

$$\mathbf{E} = -\nabla\emptyset \qquad (21)$$

If $\emptyset$ is a scalar potential, $-(\nabla\emptyset)_{\parallel} = \eta J_{\parallel}$ is the Compound of Eq. (1) and is parallel to **B** because

$$\mathbf{E} + \mathbf{v} \times \mathbf{B} = \eta\mathbf{J} \qquad (22)$$

$$\Rightarrow \mathbf{E} \cdot \mathbf{B} + (\mathbf{v} \times \mathbf{B}) \cdot \mathbf{B} = \eta\mathbf{J} \cdot \mathbf{B} \qquad (23)$$

$$\Rightarrow -\nabla\emptyset \cdot \mathbf{B} = \eta\mathbf{J} \cdot \mathbf{B}. \qquad (24)$$

Currently, since $\frac{d\emptyset}{ds} = \frac{d\emptyset}{dx}\frac{dx}{d\emptyset}$ due to the rule of the chain and $\frac{dx}{ds} = \boldsymbol{B}$, We've got

$$\frac{d\emptyset}{ds} = \nabla\emptyset \,.\boldsymbol{B} \qquad (25)$$

$$\frac{d\emptyset}{ds} = -\eta\boldsymbol{J}.\boldsymbol{B} \qquad (26)$$

and via integration along lines of magnetic fields, we may determine $\emptyset$:

$$\emptyset = -\int \eta \, \mathrm{J}.\boldsymbol{B}\, ds + \emptyset_{\mathbf{0}} \qquad (27)$$

$\emptyset_\circ$ is a fixed of integration.

Be aware that while $\emptyset_0$ must be kept separated from s, it perhaps a function of x_0, y_0, z_0, i.e., It might differ between one field line to another. by replacement the Eqs. (15,16,17)) into the integrand of Eq. (27), This integration may be used to get $\emptyset(\boldsymbol{X}_0, s)$. After this is finished, we use Eqs. (18,19,20) to drive out s, x_0 and y_0 to gain$\emptyset(\boldsymbol{X})$, handling z_0 as a constant (see below). From there, one may determine the electric field from Eq. (21) after which It is found the Plasma speed orthogonal to the magnetic field to determined, $\mathbf{V}_\perp$, via utilizing the product of the vector of Eq. (4) including **B** to profit

$$V_\perp = \frac{(\boldsymbol{E}-\eta\boldsymbol{J})\times\mathbf{B}}{\boldsymbol{B}^2} \qquad (28)$$

$\boldsymbol{v}_\parallel$is random since $(\boldsymbol{v}_\parallel\widehat{\boldsymbol{B}}) \times \boldsymbol{B} = 0$(where$\widehat{\boldsymbol{B}}$ is a unity vector spanning **B)**. Here and now, to look at the characteristics of magnetic reconnection in a completely 3D. structure, we enforce a spatially localized dispersal area. in 3D. In terms of astrophysical plasmas, this is the situation, they are recognized as being practically perfect, except for extremely tiny areas where energy release takes place. It is decided to locate the diffusion zone directly around the null point, consistent with other research findings that shearing movements often concentrate current at the null (Rickard and Titov, 1996); (Pontin and Galsgaard, 2007); (Pontine al., 2007) [20], [21],[22]. We consider the Specific resistance to be localized and adopt it as of the form.

$$\eta = \eta_0 \begin{cases} f(R,z) & R < a, \quad (z^2)^{\frac{2k}{k+1}} < b^2 \quad ,k \geq 1 \\ 0 & otherwise \end{cases} \qquad (29)$$

With $f(R,z) = ((\frac{R}{a})^2 - 1)^2 \; (\frac{(z^2)^{\frac{2k}{k+1}}}{b^2} - 1)^2$

Where $R = \sqrt{(x^2)^k + (y - jz/(2k+1))^2}$

Where η_0, a and $b \in R^+$. This is meant to help to localize the product. ηJ, therefore the diffusion area, as we haven't figured out how to use localized **J** with our analytical approach yet. It is not anticipated that the precise mathematical representation of η will impact the solution's qualitative structure. It was selected to make the equations tractable. The localization of the diffusive term η**J** is an essential characteristic for the solution's structure. (The dependency of η on k is It was select different from for k ≥ 1).

to make sure (x, y, z) is always differentiable, is chosen to keep things consistent in the way that the size of the spreading area in the x-direction is based on k. This turns out to be a crucial characteristic. Here η_0 corresponding to η at the null point, and the cylinder-shaped spreading area is oriented with esteem to the spine axis. Extends to

$z = \pm b^{(k+1)/2k}$ when $k \geq 1$

When k = 1, the diffusion region's cross-section in the z = 0 plane is circular, with radius a. but when k$\neq 1$ it extends to $x = \pm a^{1/p}$ and $y = \pm a$ to integrate Eq. (27), We must decide which surface to begin our integration on. (i.e., on which to set s=0) that only ever crosses each field line once. (See figure 3),

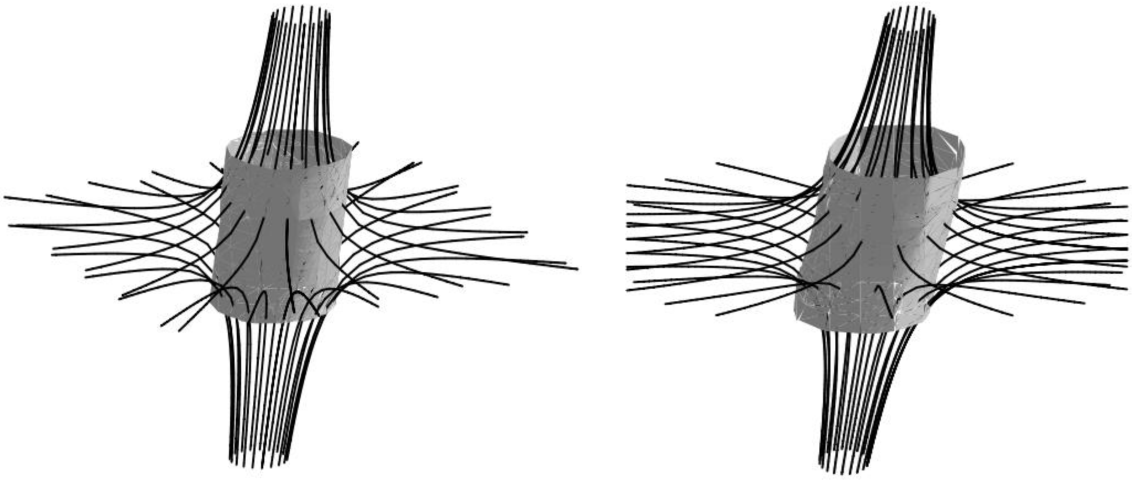

(i) (ii)

Figure 3: The superficies of η with a variety of k: (i) k = 1, (ii) k = 2 where each field line cuts over the superficial just one, for j = b = a = 1.

To guarantee that ∅ is single valued. Surfaces are selected both over and under the fan's surface, z = $\pm z_0$, constant. In order to make the mathematical formulas simpler, we presume generalization, we presume. $z_0 = b$**.** carrying out the computation of $\emptyset(\boldsymbol{X})$ as explained above provides two ways of expressing ∅, for z > 0 also z < 0. In order for these 2 formulations to coincide at the fan plane, ∅ must be continuous and smooth, therefore deemed appropriate physically, the value of ∅has to be set at $z = \pm z_0$ (i.e.,$\emptyset_0$ in Eq. (27)) to be

$$\boldsymbol{\emptyset_0} = \frac{\boldsymbol{2B_0}}{\boldsymbol{L(k+1)}} \frac{\boldsymbol{\eta_0 j}}{\boldsymbol{\mu_0}} \boldsymbol{x_0} \left(\frac{1}{(8k-1)} b^{\frac{4(k-1)}{k+1}} - \frac{2}{(4k-1)} b^{\frac{2(k-1)}{k+1}} - 1 \right), k \geq 1 \qquad (30)$$

Now $\emptyset(\boldsymbol{X})$,**E** and $\boldsymbol{V}_\perp$ is obtainable from (21), (27) and (28), as previously stated A symbolic computing package can be used to calculate the mathematical expressions, which are too long to display here. The instructions used in this example are from Appendix A.1, and we used (Maple v.12).

4. SOLUTION PROPERTIES

4.1 Reconnection nature

The plasma speed ($\boldsymbol{v}_\perp$) orthogonal to the magnetic field will be investigated to identify the magnetic reconnection process's structure. The magnetic flow is transported outer of the spreading zone at this pace. The spine is not moved in the path of x by the flow. ($v_{\perp x}(0, y, z) = 0$), hence that $v_{\perp x}$ has little bearing on the process of reconnecting. On the other hand, the plasma stream passes the fan furthermore the spine in the yz-plane. Keep in mind that this scenario is qualitatively identical to the one that is explained by (Pontin *et* al. 2005) in the situation of k = 1[16]. Figure 5 depicts the characteristics of the plasma stream on a constant x plane including various quantities of k. From this the consensus on the standstill point's fundamental structure isn't greatly influenced via changing the values of k. Nonetheless, the overall pattern indicates that when k approaches zero, As seen in (Figure 4), The plasma flow becomes less powerful across the fan surface. We'll talk about this behavior again below.

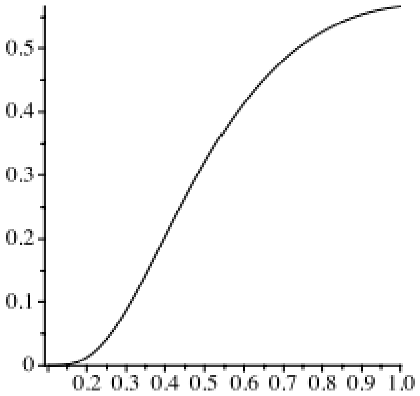

Figure 4: **$v_z$flow with k, for η_0 = η = B_0 = a = b = L = j = 1, y =1 and x = z =0.**

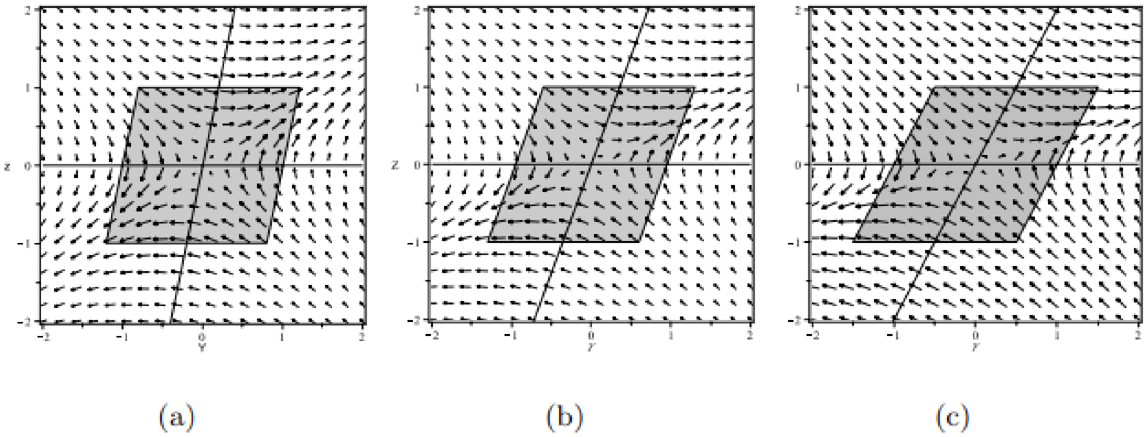

Figure 5: **The arrows represent the plasma flow through the spine and the propeller (indicated by dark lines) at an exemplary constant level x = 0, The spreading zone is marked in grey for (a) k = 2, (b) k = 0.9, (c) k = 0.5, for considerations η_0 = B_0 = j = η = b = a = L = 1.**

4.2 rate of the reconnection

It is well acknowledged that many distinct kinds of explosive astrophysical events are fundamentally caused by magnetic reconnection, Solar flares are an example of this. The reconnection rate's determinant, however, remains a significant issue and a crucial component of every reconnection paradigm, Three-dimensional rate of reconnection is described by maximal Quantity of

$$F = \int E_{\parallel}\, dl, \tag{31}$$

over every field line pass through a locally concentrated spreading area **D** (*e*.g., Schindler *e*t al.,1988) With Analog, in this situation [17].

$$F = \int_{c_2} E_{\parallel}\ dl, \tag{32}$$

where, as seen (in Figure 6), over the x-axis the curve c_2 lies. a flux surface is the fan; hence, it is also possible to compute the integral along curve c_1, situated in the fan in a direction orthogonal toward **B**. view (Figure 6). now, given that curvature c_1 is outside of D, and so, over its ($\mathbf{v} \times \boldsymbol{B} = -\boldsymbol{E}$), We are able to write

$$F = -\int_{c_1} \boldsymbol{v}\ \times \boldsymbol{B}\ .dl\ , \tag{33}$$

This makes it evident that this reconnection rate gauges how quickly flux is carried by the flow in the optimum area over the fan surface. (Pontin et al.,2005) [16].

As of Eq. (31), we possess

$$F = \int_{-a^{1/b}}^{a^{1/b}} E_x \; dx$$

$$= \frac{2B_0}{L(k+1)} \frac{\eta_0 j}{\mu_0} \left(2a \left(1 + \frac{a^{4(k-1)}}{(4k+1)} - \frac{2a^{2(k-1)}}{(2k+1)} \right) \right) \qquad k \geq 1 \qquad (34)$$

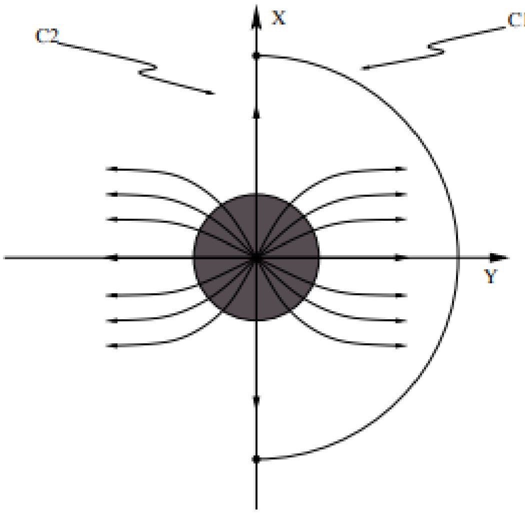

Figure 6: **The Stocks represent the field lines' orientation, and the gray area represents the propagation region, wherec_1, c_2 they connect Two points happening the x axis**.

Take observe as a means of confirmation This really sums up to the phrase discovered by (Pontin *e*t al. 2005) at what time k = 1[16]. hither, In Figure 7, we can see two separate cases where the reconnection rate is parameter dependent k. first, we put the variable j to make it constant, $j = 2j_0$ say, it produces a current that depends on k. Next, we examine the scenario in which we set $j = j_0(k+1)$, in order for the current $(\mathbf{J} = 2B_0 j/(L(k+1))\hat{X})$ is separate of k. Additionally, we will think about the impact in every one of these instances. of choosing several Quantities for parameter a, this regulates the diffusion region's dimensions. in every one of these cases the diffusion zone has a circular cross-section in any z-constant plane and is symmetric for any k when a=1. However, as stated above, each of the three coordinate axes is intersected by the diffusion region's border at

$$x = \pm a^{1/k}, y = \pm a\,, z = \pm a^{(k+1)/2k} \qquad k \geq 1 \qquad (35)$$

Thus, In the xy-plane, the diffusion area consequently becomes asymmetric when $a \neq 1$ and $k \neq 1$. Later, this trait will prove to be beneficial when compared to the outcomes of a numerical simulation.

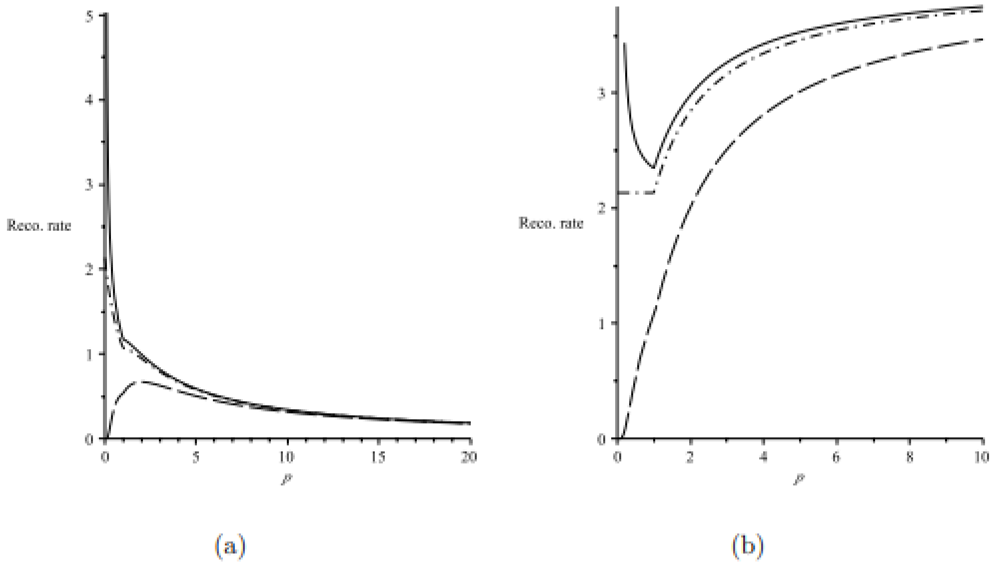

Figure 7: The pace of reconnection dependence on k, for a = 0.5 (long dashed), a = 1 (punctate), a = 1.5 (solid curve), to (a) j=$2j_0$, (b) j=$j_0(k+1)$, $\eta_0 = B_0 = j_0 = \eta = L = b = 1$

Reconnection pace as k → ∞

The diffusion zone becomes almost symmetric (or perfectly symmetric if a = 1) as k approaches infinity, as seen in equation (35). For any value of a, the following is true. Regarding the two options for our parameter j's dependency that were mentioned previously, evaluating Eq. (34) we find

$$\lim_{p\to\infty} F\Big]0_{j=2j_0} = 0$$

$$\lim_{p\to\infty} F\Big]_{j=j_0(k+1)} = \frac{4j_0B_0\eta_0}{L\eta}$$

Let us first examine the scenario in which parameter j is selected as a constant.$j = 2j_0$ so that the current $\boldsymbol{J} = 4B_0j_0/(L(k+1)\eta)\widehat{\boldsymbol{X}}$. In this case the magnetic field is $\boldsymbol{B} \to (2B_0/L)(0, y, -z)\ as\ \ k \to \infty$. In other words, the predicted outcome (F → 0) is due to the zero-current magnetic field near a 2D X-point structure.

Conversely, the reconnection pace becomes close to constant, limited value as $k \to \infty$ when $j = j_0(k+1)$(so that $\boldsymbol{J} = 2B_0j_0/L\eta\widehat{\boldsymbol{X}}$). In this case the magnetic field is $\boldsymbol{B} \to (2B_o/L)\ (0, y - j_0z. -z)$. So the setup is a 2D X-point with a constant current which is proportional to$\boldsymbol{j_0}$. As the diffusion region's size is limited along the current's ($\widehat{\boldsymbol{X}}$) direction, The Rate of connection is limited. Observe that it is proportionate to the parametersη_0, B_0/L, and j_0 as predicted. Where $2B_0j_0/L\eta$is the current modulus and η_0 is the resistivity at the null.

5. CONCLUSIONS

This chapter examines the influence of the magnetic field's symmetry at the solitary null point during magnetic reconnection. Our focus is on the 3D null point reconnection's "spine-fan mode." (Priest and Pontin, 2009) [17]. We discussed a stable solution to certain resistive MHD formulae in this chapter. The magnetic null point has been stated via **B** $= \frac{2B_0}{L(k+1)}(x, ky - jz, -(k+1)z)$ In this field, the current is Collimated to the surface of the water, in the nongenetic symmetrical Instance k = 1(recurrent eigenvalues) investigated this situation (Pontin et al. 2005)[16]. We use k as a parameter in this work. Consequently, since this steady-state kinematic solution does not take the dynamics of the system into account, a current is imposed, This, As shown by the simulations, has the same direction at the null, it has been shown that the direction of j at zero is the basic quantity for knowing the reconnection operation's magnetic nature

(Pontin *et* al., 2004, 2005) [15][16]. We intentionally imposed a localized resistivity around the null to create a localized diffusion area. In the identical case, the results are identical regarding the nature of the reconnection operation and the nature of the plasma Stream, and it that we concluded. More specifically, for all values of k, we observed plasma Stream crosswise the null's fan plane and spine line. However, based on the factors we choose, the findings mentioned above demonstrate that the reconnection rate and the diffusion area dimension may rely on the field's imbalance (k) in a variety of ways. Next, we will discuss emulation in the resisting MHD domain in the next chapter to see if any of these relationships is important in a plasma that is changing dynamically all the time.

References

[1] Sweet, P. A. (1958). The neutral point theory of solar flares. In Electromagnetic phenomena in cosmical plasmas, pages 123–134. Cambridge University Press, Cambridge

[2] Parker EN 1957 J. Geophys. Res.62PP.509–520

[3] Parker, E. N (1963) ApJ...138.552P Kinematical Hydromagnetic Theory and its Application to the Low Solar Photosphere. Astrophysical Journal, vol. 138, p.552

[4] Petschek, H. E. (1964). Magnetic field annihilation, pages 425–439. NASA SP-50, Washington, D.C.

[5] E. N. Parker. (1983 January 15). MAGNETIC NEUTRAL SHEETS IN EVOLVING FIELDS. II. FORMATION OF THE SOLAR CORONA. The Astrophysical Journal, 264:642-647,

[6] Xiao, C. J., Wang, X. G., Pu, Z. Y., Zhao, H., Wang, J. X., Ma, Z. W., Fu, S. Y., Kivelson, M. G., Liu, Z. X., Zong, Q. G., Glassmeier, G. H., Balogh, A., Korth, A., Reme, H., and Escoubet, C. P. (2006). In situ evidence for the structure of the magnetic null in a 3d reconnection event in the earths magnetotail. Nature Phyis, 2:478483

[7] Al-Hachami, A. K. and Pontin, D. I. (2010). Magnetic reconnection at 3D null points: effect of magnetic field asymmetry. Astronomy and Astrophysics, 512: A84.

[8] Priest, E. R. and Forbes, T. G. (2000). Magnetic reconnection: MHD theory and applications. Cambridge University Press, Cambridge

[9] Hornig, G. and Schindler, K. (1996). Magnetic topology and the problem of its invariant definition. Phys. Plasmas, 3:781–791

[10] Hornig, G. and Priest, E. R. (2003). Evolution of magnetic flux in an isolated reconnection process. Phys. Plasmas, 10(7):2712–1721

[11] Hornig, G. (2001). An introduction to the geometry and topology of fluid flows, pages 295–313. Kluwer, Dordrecht.

[12] Priest, E. R., Hornig, G., and Pontin, D. I. (2003). On the nature of three-dimensional magnetic reconnection. J. Geophysics. Res., 108(A7):1285

[13] Wilmot-Smith, A. L., Hornig, G., and Priest, E. R. (2006). Dynamic non-null magnetic reconnection in three dimensions. i. particular solutions. Proc. RSoc. A, 462:28772895

[14] Al-Hachami, A. K. (2019), Magnetic Reconnection in the Absence of Three-Dimension Null Point**.** Herald of the Bauman Mosco state Technical University. (6), 50-66

[15] Pontin, D. I., Hornig, G., and Priest, E. R. (2004). Kinematic reconnection at a magnetic null point: Spine-aligned current. Geophys. Astrophys. Fluid Dynamics, 98:407428.

[16] Pontin, D. I., Hornig, G., and Priest, E. R. (2005). Kinematic reconnection at a magnetic null point: Fan-aligned current. Geophys. Astrophys. Fluid Dynamics,99:7793

[17] Priest, E. R. and Pontin, D. I. (2009). 3d null point reconnection regimes. Phys. Plasmas, 16:122101

[18] Schindler, K., Hesse, M., and Birn, J. (1988). General magnetic reconnection, parallel electric elds, and helicity. J. Geophys. Res., 93(A6):55475557.

[19] Parnell, C. E., Smith, J. M., Neukirch, T., and Priest, E. R. (1996). The structure of three-dimensional magnetic neutral points. Phys. Plasmas, 3(3):759770

[20] Rickard, G. J. and Titov, V. S. (1996). Current accumulation at a three-dimensional magnetic null. Astrophys. J., 472:840852.

[21] Pontin, D. I. and Galsgaard, K. (2007). Current ampli cation and magnetic reconnection at a 3d null point. physical characteristics. J. Geophys. Res.,112: A03103

Pontin, D. I., Bhattacharjee, A., and Galsgaard, K. (2007). Current sheet formation and non-ideal behavior at three